2009-01-0433

Application of System Identification for Efficient Suspension Tuning in High-Performance Vehicles: Full-Car Model Study

Chris Boggs, Mehdi Ahmadian and Steve Southward
Virginia Institute for Performance Engineering and Research (VIPER)

ABSTRACT

One popular complement to track testing that successful race teams use to better understand their vehicle's behavior is dynamic shaker rig testing, such as 7-post and 8-post testing. Compared to track testing, rig testing is more repeatable, costs less, and can be conducted around the clock. While rig testing certainly is an attractive option, an extensive number of tests may be required to find the best setup. To make better use of rig test time, more efficient testing methods are needed. One method to expedite rig testing is to use rig test data to perform system identification and generate a model of the experiment, which may then be applied to identify potential gains for further rig study.

This study develops a system identification method for use in rig testing, using data generated from a known physical model. The results show that this method can be used to accurately predict sensor response during an 8-post test for different shock selections. Future work will apply the model developed in this study to a car tested on an 8-post rig and to perform shock selection.

INTRODUCTION

During a 7-post or 8-post rig test, the tires are supported by 4 actuated wheel platforms, or wheelloaders, that simulate inputs from the track surface. Three or four actuators, or aeroloaders, attach to the vehicle's chassis to provide forces which simulate the effect of inertial and aerodynamic forces present during a track test. The vehicle is shaken on the rig to simulate how the car would respond at a particular track or to characterize the vehicle response to more general waveforms such as sine waves or broadband signals. An example car on an 8-post rig is shown in Figure 1.

The performance of the different setups is compared by calculating a series of performance metrics. These metrics are typically used during rig tests to help summarize how the shock selection affects various aspects of vehicle behavior including mechanical grip, aerodynamics, suspension travel, and suspension loading.

Figure 1. Synergy Racing car on 8-post rig

This sensitivity information is one of the main products of the rig test. The team will use this information to help select or eliminate potential shock packages to try on the race track, and will use the sensitivity information to help make adjustments based on how the vehicle performs on the track.

The main goal of this research is to accurately predict this sensitivity information using simulations, which can augment knowledge gained from rig testing. To create an accurate model for these simulations, we will use rig test data to perform system identification, which will produce a vehicle model.

This paper develops the ID methods that may then be applied to rig test data. The first section develops the equations of motion for a linear 7 DOF vehicle model. This model treats the nonlinear shock model force as an input to a linear dynamic system, allowing us to apply linear system identification techniques. This linear vehicle model may then be coupled with nonlinear dynamic shock models to create simulated rig data sets generated using a known system model.

The methods required to perform the system ID are then discussed and applied to the simulated test data. The results of the ID are compared with the theoretical response to verify that the ID process is working properly.

To verify that the method will produce a model that will accurately simulate the response of the original model, results from the original model and the identified model are compared for multiple shock selections.

BACKGROUND

Before developing the system identification method, background information is provided on 7-post/8-post testing and the use of experimental data to improve simulation studies.

7-POST/8-POST TESTING - Due to the highly competitive nature of racing, very little of the work done in 7-post and 8-post testing has been published. Kelly et al. discusses the use of linear FRF estimates to develop track drivefiles [1]. Kowalczyk uses a linear 7 degree of freedom vehicle model to help identify tradeoffs and determine realistic limitations of tuning [2]. Kasprzak used a half-car model to help find potential gains for further exploration on a 4-post rig with soft springs attached to the chassis to simulate downforce [3]. Each of these papers successfully used linear models to aid in rig testing.

EXPERIMENTAL DATA FOR SIMULATION - To evaluate a given model's accuracy in predicting experimental results, it is common practice to use experimental data to validate the model accuracy. If desired, the model can also be updated to better match the experimental data. This process of model validation and updating can be performed on the component level, the system level, or both depending on the application. Some relevant examples showing trends applying experimental data to model validation and updating are shown below.

In the automotive industry, vehicle models are quite commonly used early in the development cycle when vehicle data is not available. This makes model updating using vehicle system data impractical, so the focus is often on assembling vehicle models from validated component models. Vilela correlated proving ground data collected for a selection of different proving ground tests with a detailed ADAMS model assembled using validated component models [4]. The correlation was determined to be acceptable, indicating that the model could have been used before the vehicle was manufactured.

Often, vehicle-level test data for an existing vehicle is used to refine a vehicle model, which will be used in future studies. The experimental data is often assumed to be the ideal response for the model to try to achieve, although experimental errors can make this a poor assumption. One basic method to use test data to update models is to first perform a parametric study to determine the sensitivity of modeling error to model parameters. The model parameters can then be adjusted using the sensitivity information to reduce modeling error [5].

A more systematic method for model updating is to apply optimization methods to find parameter values that minimize some measure of the model error. Hu performed model validation and updating on a half-car ride model using proving ground data [6]. The initial guess at the parameters was defined using component tests, which were then updated to better match the proving ground data using optimization of modeling error.

While many studies use proving ground data for model development, there has been an increasing trend to use laboratory test data since the experiments are run in a more controlled environment with higher repeatability [7]. For example, Cheli and Sabbioni performed 4-post testing on a van to identify the unknown stiffness, damping, and inertial parameters [8]. The parameters were optimized to best fit the experimental data using nonlinear optimization. Further experiments were performed to show that there was acceptable correlation between the model and data. The ability of the model to predict the effect of changing parameters was not discussed.

Most model updating studies attempt to match the displacements and/or accelerations of the sprung and unsprung masses. One additional sensor measurement that is important for a rig testing model to predict is the tire normal force. Ziegenmeyer optimized the parameters of a linear quarter-car model to minimize the

prediction error for quarter-car rig test [9]. The model was then used to predict the acceleration of the sprung mass, the unsprung mass and tire normal force with reasonable accuracy.

The above studies all use structural dynamic models to model vehicle behavior, where the models have been constructed using components that have a specific physical meaning, such as masses, springs, dampers, and their geometrical configuration. Many applications do not require accurate estimation of the structural parameters, only a model of the input-output behavior. If this is the case, a more generic dynamic model structure can be used, such as a state-space or transfer function model. These modeling structures have more modeling freedom, allowing them to account for more complex behavior, such as chassis flexible body modes. These models can be identified using generic system identification tools. By using a generic input-output model structure, there is no need for prior knowledge of the geometry of how components in the physical system are arranged or the boundary conditions for their connections. This makes them useful for quickly generating models from test data with minimal model development effort.

This paper will focus on developing a generic linear dynamic model from simulated rig test data that will allow us to predict the sensor response for different drivefiles and shock selections. Prior research by the authors has shown this method to successfully predict the response of a laboratory quarter-car rig [10].

Extending this method from the ideal simulation environment in this work to 8-post rig test data will present nonlinearities which will degrade the performance of this method. Potential sources of nonlinearity include tire separation, coil bind, coil separation, progressive spring rates, bump stops, nonlinear motion ratios, tire and joint friction, and play in the suspension.

Despite these potential nonlinearities, there are several reasons to suggest that the linear model developed here may be a useful approximation of an 8-post rig test. First, linear modeling has already been used to model the response of a rig test with positive results [1-3]. Second, the weight of the vehicle and aeroloader downforce will act to preload the tires, reducing the amount of time that the tires will separate from the wheelloaders. Third, suspension joint friction and slop will often be minimal to provide good handling. Finally, the RMS-based response measures commonly used for analysis are gross dynamic measures of the response, so even our model does not match the true response exactly, it is still possible that our RMS trends will match.

Future work will apply this method to actual 8-post rig data to determine if this model can be successfully used to predict the results of 8-post rig tests.

FULL-VEHICLE MODEL

This section develops the equations of motion for a linear full-vehicle model, where the nonlinear shock model force is treated as a feedback input to a linear dynamic vehicle model. This allows us to decouple the nonlinear shock models from the linear vehicle model and apply linear analysis to better understand the effect of shock selection on vehicle performance.

STATE-SPACE MODEL - A diagram for the 7 degree of freedom model used for this study is shown in Figure 2. The coordinate system is chosen about the center of gravity, which lies a distance a behind the front axle. We assume the center of gravity to lie along the vehicle centerline and the front and rear track widths to be equal. The influence of external forces applied to the 3 DOF chassis model by the aeroloaders may be represented as a heave force, roll moment, and pitch moment. At each corner, there is a suspension, which consists of a linear spring and an arbitrary shock force. The tire is modeled as a point mass, linear tire stiffness, and a single point tire input.

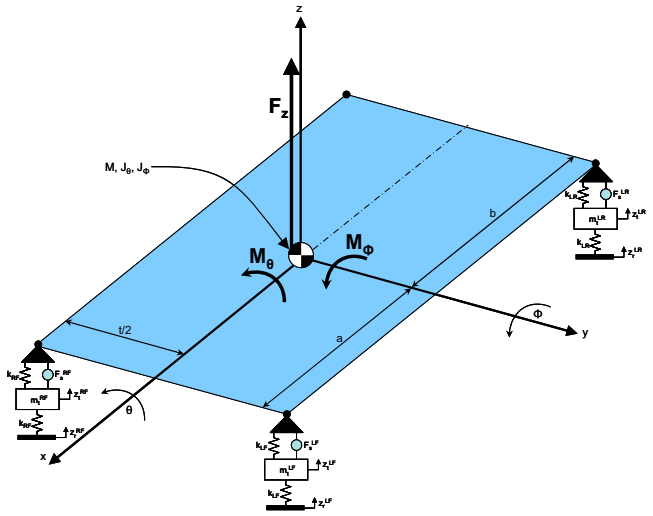

Figure 2. 7 degree of freedom vehicle model

The displacement of the four corners of the chassis, $z_{corners}$, may be expressed in terms of the chassis heave, roll, and pitch (Φ) by the transformation

$$\begin{bmatrix} z_{corner}^{LF} \\ z_{corner}^{RF} \\ z_{corner}^{LR} \\ z_{corner}^{RR} \end{bmatrix} = \begin{bmatrix} 1 & \frac{t}{2} & -a \\ 1 & -\frac{t}{2} & -a \\ 1 & \frac{t}{2} & b \\ 1 & -\frac{t}{2} & b \end{bmatrix} \begin{bmatrix} z \\ \theta \\ \phi \end{bmatrix} \qquad (1)$$

$$z_{corners} = T\Phi$$

Where *a* and *b* define the position of the front and rear axles in relation to the chassis center of gravity, while *t* defines the track. Similarly, the suspension forces applied to the four corners of the chassis, $F_{suspension}^{\Phi}$, may be expressed as an applied heave force, roll moment, and pitch moment ($F_{suspension}$) using the transformation

$$\begin{bmatrix} F_{suspension}^{z} \\ M_{suspension}^{\theta} \\ M_{suspension}^{\phi} \end{bmatrix} = \begin{bmatrix} 1 & 1 & 1 & 1 \\ \frac{t}{2} & -\frac{t}{2} & \frac{t}{2} & -\frac{t}{2} \\ -a & -a & b & b \end{bmatrix} \begin{bmatrix} F_{LF} \\ F_{RF} \\ F_{LR} \\ F_{RR} \end{bmatrix} \qquad (2)$$

$$F_{suspension}^{\Phi} = T^T F_{suspension}$$

Summation of forces and moments on the chassis yields

$$J_C \ddot{\Phi} = F_{suspension}^{\Phi} + F_A \qquad (3)$$

where I_C is a 3x3 diagonal matrix containing the chassis inertial properties, while F_A is a 3x1 vector of the forces and moments applied to the chassis to simulate aerodynamic and inertial loading. Summation of forces on the four tires yields

$$M_t \ddot{z}_t = -F_{suspension} + F_{tires} \qquad (4)$$

where M_t is a 4x4 diagonal matrix containing the four tire masses and z_t is the tire vertical displacement. The suspension and tire forces, $F_{suspension}$ and F_{tires}, are defined to be positive in compression and may be written as

$$F_{suspension} = K_s \left(z_t - z_{corners} \right) + F_S \qquad (5)$$

$$F_{tires} = K_t \left(z_r - z_t \right) \qquad (6)$$

Substituting Equations 1-4 into Equations 5-6 yields the equations of motion

$$\begin{bmatrix} J_C & 0_{3x4} \\ 0_{4x3} & M_t \end{bmatrix} \begin{bmatrix} \ddot{\Phi} \\ \ddot{z}_t \end{bmatrix} + \begin{bmatrix} T^T K_s T & -T^T K_s \\ -K_s T & K_s + K_t \end{bmatrix} \begin{bmatrix} \Phi \\ z_t \end{bmatrix} = \begin{bmatrix} I_3 & 0_{3x4} & T^T \\ 0_{4x3} & K_t & -I_4 \end{bmatrix} \begin{bmatrix} F_A \\ z_r \\ F_s \end{bmatrix} \qquad (7)$$

$$M\ddot{Z} + KZ = Lu$$

The equations of motion can be rewritten in state-space form as

$$x_1 = Z, \; x_2 = \dot{Z}$$

$$\begin{bmatrix} \dot{x}_1 \\ \dot{x}_2 \end{bmatrix} = \begin{bmatrix} 0_{7x7} & I \\ -M^{-1}K & 0_{7x7} \end{bmatrix} \begin{bmatrix} x_1 \\ x_2 \end{bmatrix} + \begin{bmatrix} 0 \\ M^{-1}L \end{bmatrix} u \qquad (8)$$

$$\dot{x} = Ax + Bu$$

In addition to defining the dynamic equations, sensor response may be defined by an output equation of the form

$$y = Cx + Du \qquad (9)$$

Output equations are formed for shock velocity, tire force, ride height, suspension deflection, chassis acceleration, wheel acceleration, and spring forces.

The model parameters used are shown in Table 1. The sprung and unsprung masses correspond to a 3000 lb car with 85% sprung mass, and 45% of the unsprung mass in the front. The roll and pitch inertia are 40% and 60% of the track and wheelbase, respectively. The suspension and tire stiffnesses are within the range of typical values. While these parameters do not neccesarily reflect those of a NASCAR Cup car, they do describe a vehicle whose behavior is qualitatively similar, making it sufficient for ID method development.

Table 1. Model Parameters

Track Width	70	in
CG-Front Axle	60	in
CG-Rear Axle	50	in
Sprung Mass	2550	lbm
Roll Inertia	1.5E+06	lbm-in^2
Pitch Inertia	5.5E+06	lbm-in^2
Front Unsprung Mass	101	lbm
Rear Unsprung Mass	124	lbm
Front Spring Rate	1280	lbf/in
Rear Spring Rate	588	lbf/in
Tire Stiffness	2000	lbf/in
Linear Damper	30	lbf/(in/s)

FREQUENCY RESPONSE - The general behavior for the linear portion of the vehicle model may be summarized by the frequency response. These plots provide insight on system behavior, which can be applied during the identification process. The frequency response may be calculated by talking the Laplace transformation of Equation 8 and substituting it into Equation 9

$$\begin{aligned} y(s) &= \left[C(sI - A)^{-1} B + D \right] u(s) \\ &= H(s) u(s) \\ &= H_{rig}(s) u_{rig}(s) + H_{shocks}(s) u_{shocks}(s) \end{aligned} \qquad (10)$$

where the input vector was partitioned between inputs due to the rig actuators and inputs due to the shock forces in the last step.

For brevity we only consider the shock velocity outputs, but the trends observed here may be applied to the remaining input-output pairs. The frequency response for all four shock velocities and for three different inputs is shown in Figure 3.

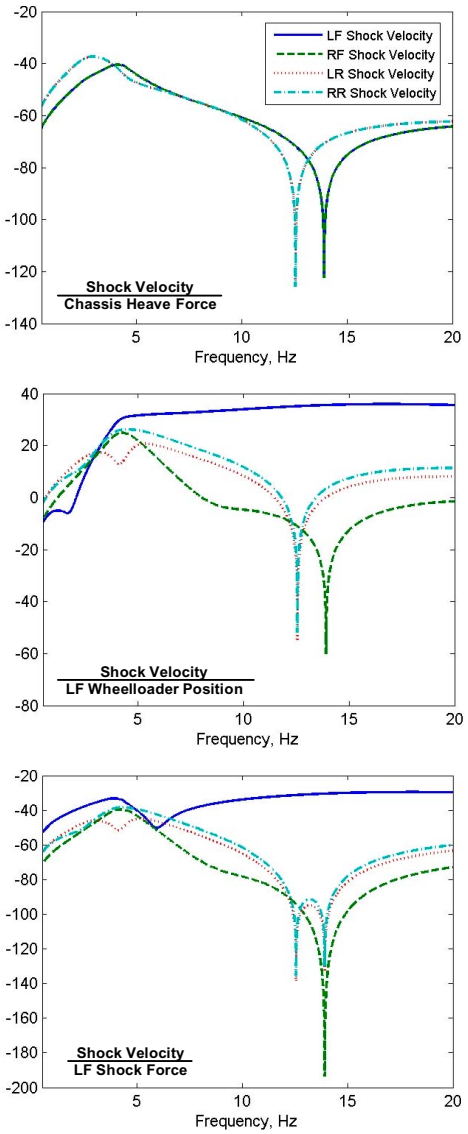

Figure 3. Shock velocity FRFs

For the chassis force input, 1000 lbs chassis heave force gives 10 in/s near resonance, and 1 in/s below 1 Hz and above 9 Hz. Further chassis velocity can be attained by aeroloader force by applying roll and pitch moments.

The left front wheelloader input creates about 1 in/s shock velocity near DC and 30 in/s shock velocity near resonance for a 1 inch left front wheelloader input. The left front shock velocity frequency response maintains a high level at higher frequencies due to the proximity of the wheelloader to the shock. All other shock velocities drop about 20 dB above 15 Hz due to the filtering effect of the chassis.

The left front external shock force produces about 1 in/s left front shock velocity for every 100 lbs. The other shock velocities have similar levels at below 8Hz, but the level drops 40 dB at higher frequencies due to the filtering effects of the chassis.

These observations can be used to assist our identification efforts. To successfully perform frequency response estimation using experimental data, we need to have significant output energy at all frequencies of interest relative to the noise level. This will provide a good signal-to-noise ratio, or coherence near 1 for a linear system. To design excitation to provide good output signal levels, the system behavior should be considered.

Notice that the chassis heave force is effective for exciting response below 5 Hz, but the response drops off at higher frequencies. This trend is also true for chassis roll and pitch moments. Conversely, the wheelloaders are ineffective at exciting outputs below 3 Hz but are useful for higher frequency excitation. Also, the most effective excitation at higher frequency will be the wheelloader closest to the sensor of interest. This suggests the need for excitation from both the wheelloader(s) closest to the sensor and the aeroloaders if we want a good signal-to-noise ratios from 1 to 20 Hz.

While it is ideal to get good signal-to-noise ratios in all output signals at all frequencies, this is often impractical due to the system's behavior, physical input limitations, and vehicle response limitations. If the output level of a particular sensor due to a particular input will always be low over a range of frequencies for the desired excitation signals to be used with the model, the poor frequency response estimation for that input-output pair in that frequency range may be replaced by a small or zero frequency response estimation with minimal reduction in model accuracy from the ideal model. Therefore, it is not critical to accurately estimate the FRF in frequency ranges that are known to have low response levels.

Notice that accurate frequency response estimation for aeroloader inputs is only critical at lower frequencies. At higher frequencies, the response is attenuated, so a poor frequency response estimate could be replaced by a small or zero frequency response to reduce modeling error.

For the wheelloader inputs and shock force inputs, the frequency response is highest near resonance and remains at a high level as frequency increases for input-output pairs that are physically located within one corner and not attenuated through the chassis. This indicates that frequency response estimation is most important for wheelloader and shock force inputs near resonance. It is also important for directly-coupled input-output pairs at higher frequencies.

This section has summarized the full-vehicle model's behavior. These results can then be applied to design excitation signals for identification tests and to modify the identification process where frequency response estimation is poor.

FULL-VEHICLE SIMULATION - Now that we have developed a full-vehicle model and explored the behavior of the model, we will now apply the model to generate data sets that can be used to develop the identification method. Since we already know the ideal model, performing identification on data generated by the model will allow us to validate our identified model with the ideal model, which will allow us to correct any issues in the identification process.

First, we need to incorporate shock absorber models developed previously into the vehicle model [11]. This is accomplished by applying the shock velocity calculated from the linear vehicle model to the nonlinear dynamic shock model, as shown in Figure 4. The shock force calculated by the shock model is then fed back as an input to the linear vehicle model using the external shock force input.

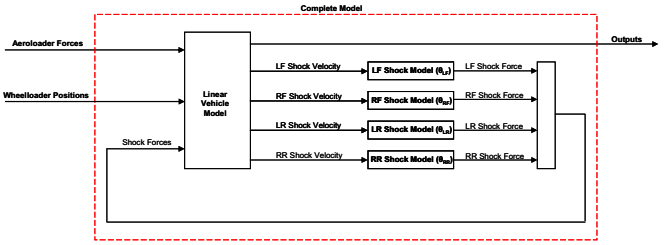

Figure 4. Coupling of vehicle and shock absorber models

This model structure can be easily implemented using Simulink. To implement the Simulink model in discrete-time, the linear vehicle model and the shock model are discretized at 100 Hz using Tustin's bilinear transformation, available in MATLAB's *c2d* function.

Five simulations were performed to generate data for use in system identification. An 800 second Gaussian bandlimited white noise drivefile was constructed to excite the Simulink model. Each signal was bandlimited from 0 to 30 Hz using an 8th order discrete-time Butterworth filter. The peak signal amplitudes were set to 1 inch for the wheelloaders and 500 lbs for the chassis heave force. The chassis roll moment and chassis pitch moment amplitudes were set to be 3 times the chassis roll and pitch stiffness respectively in in-lbs/degree. This drivefile was applied to the Simulink model to generate data that will be used to perform system identification on the linear vehicle model. One baseline simulation was performed with a linear shock with an damping coefficient of 20 lbs/(in/s) and four additional simulations were performed where the baseline damper at each corner was replaced by a nonlinear dynamic shock model with an equivalent damping coefficient of 8 lbs/(in/s).

SYSTEM IDENTIFICATION METHODS

This section presents system identification methods that will be applied to the data generated using the full-vehicle model. To analyze the identification methods, it will be convenient to represent the vehicle model derived above as shown in Figure 4. This diagram partitions the linear system that we wish to identify into the response caused by the actuators and the additional response caused by the external shock force. The shock force is defined by a feedback loop, as shown in Figure 5.

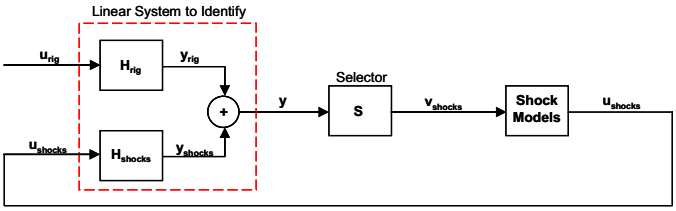

Figure 5. Diagram of system to identify

The feedback nature of the shock force input, as shown in Figure 5, will often cause straightforward FRF estimation methods to fail or to yield poor coherence. The next two sections will describe the issues with FRF estimation and one method to address theses issues.

ISSUES WITH FRF ESTIMATION - If all the inputs were independent, a common practice is to create a nonparametric estimate of the frequency response matrix, which consists of a complex number for each input, output, and frequency. For each frequency and output, we wish to fit the model

$$y = H_{rig}u_{rig} + H_{shocks}u_{shocks} \tag{11}$$

where the inputs and outputs consist of the frequency domain component for a given frequency. To fit the model, we collect several data blocks and select the model coefficients that minimize some measure of model error. Data blocks may be taken from a series of

tests or from selecting multiple blocks of data from a longer data set. The measured output in the k^{th} data block will contain some error from the ideal model's estimate, which may be written as

$$y[k] = H_{rig}u_{rig}[k] + H_{shocks}u_{shocks}[k] + \varepsilon[k] \tag{12}$$

If we collect *K* data blocks, we can arrange the results in matrix form as

$$\begin{bmatrix} y[1] \\ \vdots \\ y[K] \end{bmatrix} = \begin{bmatrix} u^T{}_{rig}[1] & u^T{}_{shocks}[1] \\ \vdots & \vdots \\ u^T{}_{rig}[K] & u^T{}_{shocks}[K] \end{bmatrix} \begin{bmatrix} H^T{}_{rig} \\ H^T{}_{shocks} \end{bmatrix} + \begin{bmatrix} \varepsilon[1] \\ \vdots \\ \varepsilon[K] \end{bmatrix}$$

$$Y = UH + E \tag{13}$$

We can choose to select our frequency response estimate to minimize the error measure

$$J = E^*E \tag{14}$$

This is a least-squares problem, whose solution satisfies the normal equations

$$\begin{aligned} \left(U^*U\right)H &= U^*Y \\ S_{uu}H &= S_{uy} \end{aligned} \tag{15}$$

To find a unique solution for the frequency response matrix *H* in Equation 15, the autospectrum matrix must be nonsingular. A necessary condition for the autospectrum matrix to be nonsingular is that the input matrix *U* defined in Equation 13 must be full rank, which is rank 11 in our case. This requires that there must be at least 11 linearly independent input block rows and 11 linearly independent input columns to solve for *H*.

For the simple case of linear shocks, we can show that the shock force inputs will be linearly dependent on the rig inputs. For linear shocks, the shock force can be written

$$\begin{aligned} u_{shocks} &= Cv_{shocks} \\ &= CSy \end{aligned} \tag{16}$$

where *C* is a 4x4 diagonal matrix whose diagonal entries contain the 4 shock damping coefficients and *S* is a matrix that selects the shock velocities out of the output vector. Substituting Equation 11 and solving for the shock force yields

$$\begin{aligned} u_{shocks} &= CSy \\ &= CSH_{rig}u_{rig} + CSH_{shocks}u_{shocks} \\ &= \left(I - CSH_{shocks}\right)^{-1} CSH_{rig}u_{rig} \\ &\triangleq H_A u_{rig} \end{aligned} \tag{17}$$

This shows that the shock force is linearly dependent on the rig inputs when the shocks are linear, so no unique solution to Equation 15 exists when this frequency response estimation is applied in a straightforward manner. Physically, this means that since the shock inputs are linearly related to the rig inputs, it is impossible to determine if the outputs are linearly related to the shock inputs or the rig inputs. This argument can be extended to shocks that exhibit linear dynamic behavior by allowing the *C* matrix to be complex.

If the shock is nonlinear, the nonlinear portion of the shock force provides some shock force excitation that is linearly independent from the rig inputs. If the nonlinear contribution is small, the output caused by the independent portion of the shock force will be small, causing poor coherence. This suggests one option to improve coherence is to use highly nonlinear shock absorbers, but it may not be practical to test with a shock with enough nonlinearity to achieve the desired model quality.

The observation that it is impossible to identify the shock input frequency response using conventional procedures and that poor coherence is expected when the shock is close to linear motivate developing alternate identification methods.

FRF ESTIMATION FOR SHOCK FORCE INPUTS - To get accurate estimates of the frequency response between shock force inputs and sensor outputs, more shock force signal energy must be linearly independent from the rig inputs. This section provides a summary of potential methods to get quality shock force input frequency response estimations.

The simplest method of applying uncorrelated shock force is to test with a highly nonlinear shock. This will only be successful if the nonlinear portion of the shock force can excite outputs with good signal-to-noise ratio and the nonlinear shock does not excite vehicle nonlinearities, invalidating the linear vehicle model assumption.

The most direct method of applying linearly independent shock force is to replace the shock with an active or semi-active suspension element and applying independent control inputs. Alternately, different control policies could be applied for different data blocks [12]. This method has the potential for good quality frequency response estimates, but it requires preparation of active or semi-active suspension members to be mounted in the place of the shocks, limiting the convenience of applying this method to an arbitrary vehicle during normal 8-post testing operations.

A convenient method motivated by the option of applying multiple control policies is to test with multiple shocks.

This method is equivalent to applying multiple control policies using an active element, where the control policy is limited by the performance that can be achieved by a passive damper. This will produce linearly independent input columns in the U matrix even if the shocks are linear.

To prove that this will allow for unique identification even if the dampers are linear, we will describe an experimental procedure that will create an input matrix that is full rank. First let us partition the shock force into a linear damper force and an additional arbitrary damper force

$$\begin{aligned} u_{shocks} &= \bar{C}Sy + \left(u_{shocks} - \bar{C}Sy\right) \\ &= \bar{C}Sy + \Delta F \end{aligned} \tag{18}$$

where $\bar{C}$ is a 4x4 diagonal matrix containing baseline linear damping coefficients that are free to be set as desired. The arbitrary portion of the damper force may be written as

$$\Delta F = \begin{bmatrix} \Delta f_1 \\ \Delta f_2 \\ \Delta f_3 \\ \Delta f_4 \end{bmatrix} = \begin{bmatrix} u^1_{shocks} - \bar{c}_1 v^1_s \\ u^2_{shocks} - \bar{c}_2 v^2_s \\ u^3_{shocks} - \bar{c}_3 v^3_s \\ u^4_{shocks} - \bar{c}_4 v^4_s \end{bmatrix} \tag{19}$$

where u^i_{shocks}, $\bar{c}_i$, and v^i_s are the shock force, baseline damping coefficient, and the shock velocity of the i[th] shock. Equation 11 can then be rewritten

$$\begin{aligned} y &= H_{rig}u_{rig} + H_{shocks}\left(\bar{C}Sy + \Delta F\right) \\ &= \left(I - H_{shocks}\bar{C}S\right)^{-1}\left(H_{rig}u_{rig} + H_{shocks}\Delta F\right) \\ &= \tilde{H}_{rig}u_{rig} + \tilde{H}_{shocks}\Delta F \end{aligned} \tag{20}$$

To identify both $\tilde{H}_{rig}$ and $\tilde{H}_{shocks}$, we need to excite both the rig inputs and the change in shock force input. Let us collect 7 baseline data sets with linear dampers whose damping coefficients are defined by $\bar{C}$. Further, let the drivefiles for all 7 data sets be linearly independent at all frequencies, such that

$$U_{rig} = \begin{bmatrix} u^T{}_{rig}[1] \\ \vdots \\ u^T{}_{rig}[7] \end{bmatrix} \tag{21}$$

is full rank for all frequencies. Since the damping force for these 7 baseline data blocks is $\bar{C}Sy$, the corresponding ΔF is zero.

Next, we collect 4 additional data sets, using alternate shock selections for each data block. For the first data block, we remove the linear left front shock and replace it with a shock with a different damping coefficient $c_1^{'}$, such that

$$\Delta F = \begin{bmatrix} \Delta f_1 \\ 0 \\ 0 \\ 0 \end{bmatrix} = \begin{bmatrix} \Delta c_1 v^1_s \\ 0 \\ 0 \\ 0 \end{bmatrix}, \quad \Delta c_1 = c_1^{'} - \bar{c}_1 \neq 0 \tag{22}$$

The arbitrary contribution of the shock force Δf_1 will be nonzero at all frequencies that v^1_s is nonzero. It is possible to excite the vehicle with a drivefile $u^T{}_1$ such that the shock velocity v^1_s is nonzero at all frequencies except at frequencies where all inputs have a zero FRF. Since the shock velocity frequency response consists of a ratio of polynomials with a numerator polynomial of order 13 or less, there will be at most 13 frequencies where the shock velocity must be zero. In practice, there will be much less frequencies where the shock velocity must be zero, and the presence of a poor FRF estimate at a few zeroes will not significantly degrade model quality.

This is repeated for the remaining 3 shock locations, where the shock at the present location is replaced by an arbitrary shock and all other shocks are the baseline shocks. Collecting the data from all 11 experiments yields the system of equations

$$\begin{bmatrix} y_0[1] \\ \vdots \\ y_0[7] \\ y_1 \\ y_2 \\ y_3 \\ y_4 \end{bmatrix} = \begin{bmatrix} & 0 & 0 & 0 & 0 \\ U_{rig} & \vdots & \vdots & \vdots & \vdots \\ & 0 & 0 & 0 & 0 \\ u^T{}_1 & \Delta f_1 & 0 & 0 & 0 \\ u^T{}_2 & 0 & \Delta f_2 & 0 & 0 \\ u^T{}_3 & 0 & 0 & \Delta f_3 & 0 \\ u^T{}_4 & 0 & 0 & 0 & \Delta f_4 \end{bmatrix} \begin{bmatrix} \tilde{H}^T_{rig} \\ \tilde{H}^T_{shocks} \end{bmatrix} + \begin{bmatrix} \varepsilon_0[1] \\ \vdots \\ \varepsilon_0[7] \\ \varepsilon_1 \\ \varepsilon_2 \\ \varepsilon_3 \\ \varepsilon_4 \end{bmatrix} \tag{23}$$

$$Y = UH + E$$

where $y_0[k]$ is the output measured for baseline shock experiment k, and y_i is the output measured from alternate shock experiment i.

Let us restrict the following analysis to frequencies where all actuator inputs do not have a zero for the current shock velocity. Since U_{rig} is full rank, the first 7 columns of the input matrix are rank 7. Since $\Delta f_i \neq 0$ the last four columns of the input matrix are rank 4. For the input matrix to be rank deficient, at least one of the last four columns must be linearly dependent on the first 7 columns. This implies that the equation

$$\begin{bmatrix} U_{rig} \\ u^T{}_i \end{bmatrix} v = \begin{bmatrix} 0_{7x1} \\ \Delta f_i \end{bmatrix} \tag{24}$$

must be satisfied for some *i*. Since U_{rig} is full rank, *v* must be zero. This requires $\Delta f_i = 0$, which contradicts Equation 22. Therefore, an experiment conducted using the above procedure will produce a full rank input matrix at all frequencies where the shock velocity is nonzero, allowing estimation of a unique frequency response estimation.

The least-squares problem defined by the data matrices in Equation 23 and the objective function in Equation 14 may then be used to solve the normal equations in Equation 15 to give the frequency response estimates for the rig inputs and the shock inputs. In practice, more than 11 data sets would be collected to allow for averaging and to provide an estimate of model quality.

In contrast to the above global estimation approach, it is often desirable to first fit a baseline model for the rig inputs, then augmenting the baseline model with component sensitivity models as needed. If the error in the baseline model is small, the results will be very similar. An advantage of this sequential approach is that it allows us to deal with smaller input matrices, making the solution more computationally efficient. Another advantage is that it allows us to calculate coherence for a single-input single-output FRF estimation for the component inputs, giving us a good indication of where the model performs well.

The sequential approach may be written as a sequential least-squares problem by partitioning Equation 23 into the rig input tests and the component input tests. The least-squares problem for the rig inputs with *K* data sets may be written

$$\min\ J = E_{rig}{}^* E_{rig}$$

$$\begin{bmatrix} y_0[1] \\ \vdots \\ y_0[K] \end{bmatrix} = \begin{bmatrix} u^T{}_{rig}[1] \\ \vdots \\ u^T{}_{rig}[K] \end{bmatrix} \tilde{H}^T_{rig} + \begin{bmatrix} \varepsilon_0[1] \\ \vdots \\ \varepsilon_0[7] \end{bmatrix} \tag{25}$$

$$y_{rig} = U_{rig} \tilde{H}^T_{rig} + E_{rig}$$

The solution to this least-squares problem satisfies

$$\left(U_{rig}{}^* U_{rig}\right) \tilde{H}^T_{rig} = U_{rig}{}^* Y_{rig} \tag{26}$$

Once the rig input frequency response has been determined, the shock input frequency responses may be estimated independently. The least-squares problem for the i^{th} shock input with K_i data sets, given the rig input frequency response, may be written

$$\min J_i\big|_{\tilde{H}_{rig}} = E_i{}^* E_i$$

$$\begin{bmatrix} \Delta y_i[1] \\ \vdots \\ \Delta y_i[K_i] \end{bmatrix} = \begin{bmatrix} y_i[1] - u_i^T[1] \tilde{H}_{rig}{}^T \\ \vdots \\ y_i[K_i] - u_i^T[K_i] \tilde{H}_{rig}{}^T \end{bmatrix} = \begin{bmatrix} \Delta f_i[1] \\ \vdots \\ \Delta f_i[K_i] \end{bmatrix} \tilde{H}_{shock_i} + \begin{bmatrix} \varepsilon_i[1] \\ \vdots \\ \varepsilon_i[K_i] \end{bmatrix} \tag{27}$$

$$\Delta Y_i = \Delta F_i \tilde{H}_{shock_i} + E_i$$

$$\Delta y_i[k] = y_i[k] - \tilde{H}_{rig} u^T{}_i[k]$$

where $\tilde{H}_{shock_i}$ is the frequency response for the i^{th} shock input. This least-squares problem satisfies

$$\left(\Delta F_i^* \Delta F_i\right) \tilde{H}^T_{shock_i} = \Delta F_i^* \Delta Y_i \tag{28}$$

This sequential procedure was applied to the data generated by simulation, providing frequency response estimates for both rig inputs and shock inputs.

While the above description assumes linear baseline shocks, this method may also be applied if all the shocks are nonlinear. If the baseline shocks are nonlinear, a system of equations similar to Equation 23 may be formed with more nonzero entries in the last 4 columns of the input matrix. Due to the additional nonzero entries in the input matrix, the equations cannot be decoupled as in Equations 25 - 28, so the entire system must be solved simultaneously.

PARAMETRIC SYSTEM IDENTIFICATION - Now that the nonparametric frequency responses have been estimated, these estimates may be used to fit a parametric model. The parametric model will have the advantages of smoothing the nonparametric frequency response, improving the model in small frequency ranges where the nonparametric model was poor, and being more efficient for simulation.

There are many different methods of performing parametric system identification, which can be chosen depending on the particular application. The transfer function for each input/output pair can be defined by its poles, zeros, and constant gain. In an ideal linear system, all input/output pairs should share the same poles and only differ by the zeros and constant gain. The identification of the system poles is often important

for applications in controls and structural parameter identification.

In our case, it is not necessary to identify a consistent set of system poles. All we want is to simplify our nonparametric frequency response estimates into a convenient transfer function relationship that will allow us to simulate the linear system more efficiently. This allows us to use a simpler method of fitting a single-input single-output (SISO) transfer function to the frequency response estimate for each input/output pair. This method will give a different set of poles, zeros, and a constant for each input/output pair. One advantage of this method is that it is very easy to fit a SISO transfer function, and many methods are readily available.

Another advantage is that it localizes error in the frequency response estimate to the corresponding transfer function estimate. If there is significant error in the frequency response estimate for one of the input/output pairs due to factors such as noise, poor excitation, nonlinearity, or sensor malfunction, the error will only affect the corresponding transfer function estimate.

The SISO method chosen for this work uses the *invfreqs* function in MATLAB [13]. This method fits a SISO transfer function of the form

$$H(s) = \frac{B(s)}{A(s)} = \frac{b_n s^n + b_{n-1} s^{n-1} + \cdots + b_0}{s^m + a_{m-1} s^{m-1} + \cdots + a_0} \tag{29}$$

by minimizing the equation-error cost function

$$J = \sum_k w_t(k) \left| h(k) - \frac{B(j2\pi f(k))}{A(j2\pi f(k))} \right|^2 \tag{30}$$

where $f(k)$ is the frequency at index *k*, $h(k)$ is the nonparametric frequency response estimate, and $w_t(k)$ is a weighting factor. This optimization problem is nonlinear in nature and must be solved using iterative nonlinear programming techniques. The *invfreqs* function uses a Gauss-Newton iterative search to solve the nonlinear programming problem.

SYSTEM IDENTIFICATION RESULTS

This section applies the identification methods with the simulated data sets to generate a model that approximates the vehicle behavior. The resulting model is then compared with the original model to determine where the ID process was successful and to help improve the ID method.

FRF ESTIMATION RESULTS - Five simulations were performed to generate data for use in system identification. An 800 second Gaussian white noise drivefile, bandlimited from 0 to 30 Hz drivefile was constructed to excite the Simulink model. One baseline simulation was performed with an empirical shock model with a damping coefficient of 20 lbs/(in/s) and four additional simulations were performed where the baseline dampers were replaced by a different empirical shock model with a damping coefficient of 8 lbs/(in/s).

The first data set was used to estimate the rig input frequency response. Forty data blocks were created from the 800 second data set using a Hamming window with 50% overlap, giving frequency resolution of 0.03 Hz. The frequency response estimates for the rig inputs was very close to the ideal frequency response, with a coherence very close to 1. The only exception was the ride height / roll moment frequency response, which had almost no response due to vehicle symmetry.

The next four data sets were used to estimate the shock input frequency response, using the same settings as the first data set. The FRF estimate and the associated coherence for the left front shock velocity output for all four shock force inputs is shown in Figure 6. The results for the left front shock velocity are consistent with the results for the other three shock velocities. For the left front shock force input, the frequency response estimate is accurate for all frequencies except near the zero at 6 Hz. For the other shock force inputs, the frequency response estimate is only good near the resonant peaks.

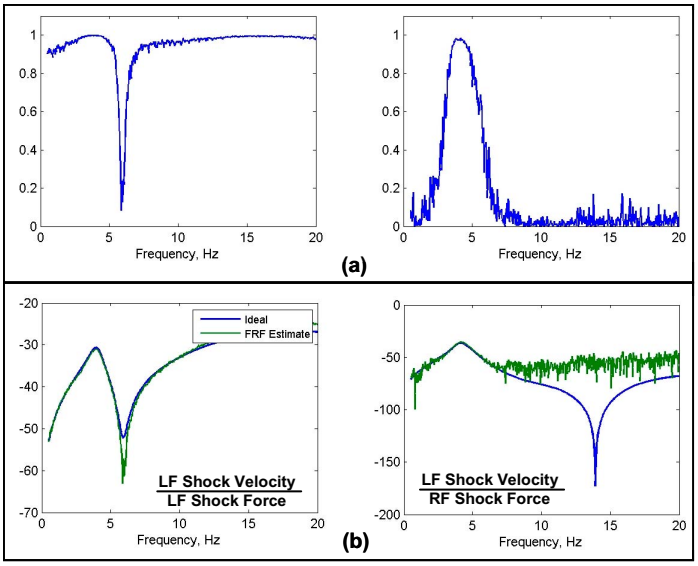

Figure 6. Shock velocity FRF estimate:
(a) Coherence, (b) FRF

In all cases, the FRF estimate is poor only where there is very low output energy, resulting in poor coherence. For Figure 6, the coherence drops when the FRF

magnitude drops below -60 dB, indicating 0.1 in/s of velocity for every 100 lbs of shock force. This is a significant observation, because if the model is poor when the response level is low, the poor frequency response estimate may be replaced by a small frequency response, which will be close to the ideal model.

Next, we show the FRF estimate and the associated coherence for the left front tire force in Figure 7, which is consistent with the other three tire forces. For the left front shock force, we see that the estimate is accurate except at lower frequencies, corresponding to the low response level. For the other shock force inputs, the estimate is accurate only near the resonance peaks.

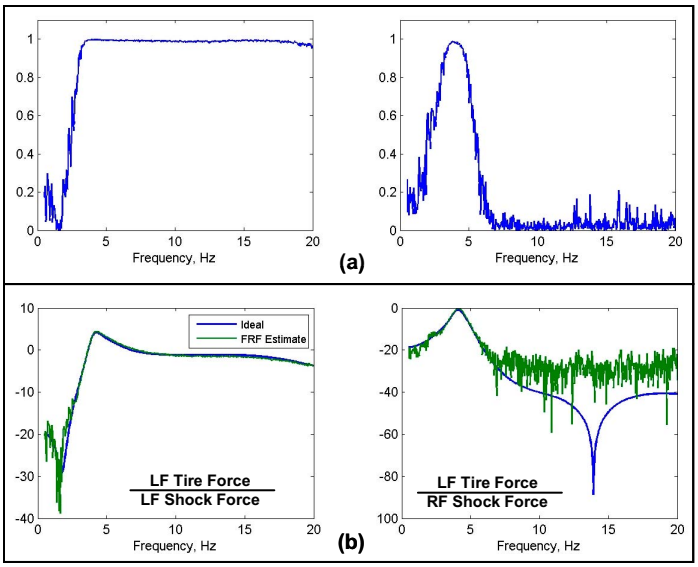

Figure 7. Shock velocity FRF estimate:
(a) Coherence, (b) FRF

Finally, we show the FRF estimate and the associated coherence for the front ride height in Figure 8, whose trends may be generalized to the rear ride height. For the front shock forces, the results are generally good except at higher frequencies, corresponding to a zero in the FRF and high frequency attenuation. For rear shock forces, the estimate is only good near the resonance.

These results have shown us that our frequency response estimates for shock force inputs are good when the response levels are high, which occurs more often for direct coupling input/output pairs that occur along a block diagonal of the frequency response matrix and for off-diagonal entries near resonance. Estimates are reasonable when the response levels are low. Also the coherence function provides a useful figure of merit for the frequency response estimates, indicating where the model will be poor.

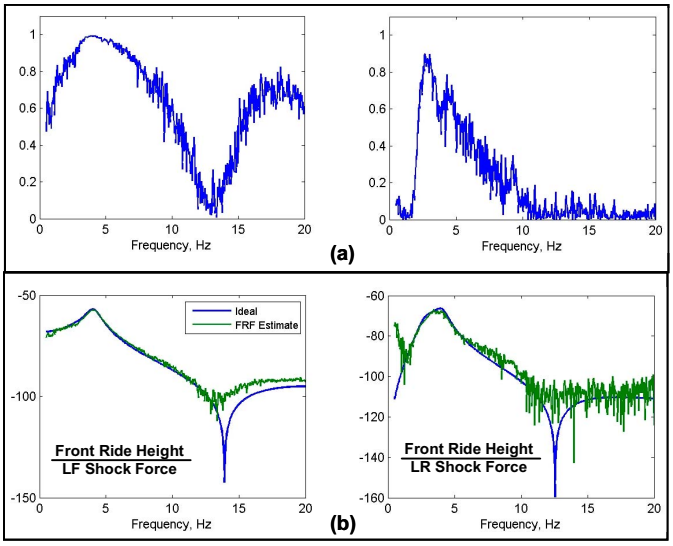

Figure 8. Ride height FRF estimate:
(a) Coherence, (b) FRF

The FRF estimates may be processed prior to parametric identification to provide better results. First, poor estimates observed for the shock force input at higher frequencies may be replaced by a residual fit of the form

$$H_{high}(f) = \frac{Ke^{j\phi}}{f^N} \tag{31}$$

This fit provides a linear dB/decade rolloff and a constant phase. The form of this residual fit is based on the assumption that the transfer function will be dominated by the highest-order nonzero terms in the numerator and denominator for these higher frequencies. A similar fit was performed at lower frequencies.

To further smooth the FRF estimate prior to parametric identification, the FRFs are lowpass filtered. Filtering a complex vector may be performed analogously to filtering a real vector, with real filters being applied to the magnitude in dB and the unwrapped phase. A 4th order Butterworth filter was constructed to attenuate FRF variations with a width of 0.6 Hz or less, corresponding to 18 frequency samples. This filter was then applied to the magnitude in dB and the unwrapped phase using the MATLAB function *filtfilt* to avoid frequency shift.

PARAMETRIC IDENTIFICATION RESULTS - Now that the nonparametric frequency response estimates have been calculated, the next step is to use these results to fit a parametric model to each input/output pair using the *invfreqs* function. The denominator polynomial orders were increased until good matching was achieved, resulting in denominator orders ranging from 6 to 8. The tire force and ride height outputs have direct feedthrough

from the nearby wheelloaders, so their numerator order is set equal to the denominator order, while all other numerator orders are set to one order lower than the denominator. A weighting function of 1 was used between 0.5 and 10 Hz, while a weighting function of 0.5 was used from 10 to 20 Hz.

The results of the parametric fit created by *invfreqs* are compared with the ideal response and the modified FRF estimate in Figure 9. As desired, all transfer function fits closely approximate the ideal FRF where magnitude is high, while the transfer function magnitudes are low when the FRF magnitude is low. While there is some disagreement at low magnitude, this will have a small influence on simulation results

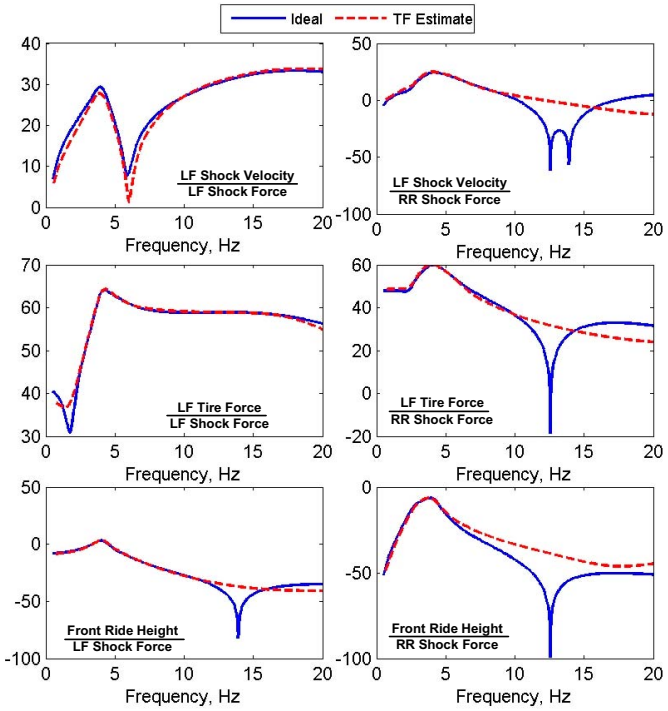

Figure 9. Results of Parametric ID

SIMULATION WITH IDENTIFIED MODEL - The identified model can now be applied to perform full-vehicle simulations using Simulink. The continuous-time transfer function model is converted to a discrete-time state space model sampled at 100 Hz using Tustin's bilinear transformation in the MATLAB function *c2d*. The shock velocity calculated as an output of the linear model is used to calculate the shock force, which is then fed back as an input to the linear vehicle model.

Five simulations were performed with the identified model to compare with simulations using the ideal model. The 800 second Gaussian white noise bandlimited to 30 Hz drivefile was used to excite the Simulink model. One baseline simulation was performed with 4 nonlinear dynamic baseline shock models with an equivalent damping coefficient of 20 lbs/(in/s) and four additional simulations were performed where the baseline damper at each corner was replaced by a nonlinear dynamic shock model with an equivalent damping coefficient of 8 lbs/(in/s).

The results from each simulation were bandpass filtered from 1 to 20 Hz using a 4th order Butterworth filter. A comparison of the tire force and front ride height using the ideal model and the identified model with the baseline shocks, the left front shock changed, and the right front shock changed is shown in Figure 10. These plots show that the simulation using the ID model match the original data well. Errors in ride height are small, while there is good matching of the tire force at the dominant frequency band of 3-5 Hz. Peak errors in ride height occur when the signal is changing rapidly, suggesting phase error. The largest error occurs with the left front tire force when the left front shock is changed, where the error magnitude is roughly 25% of the signal level.

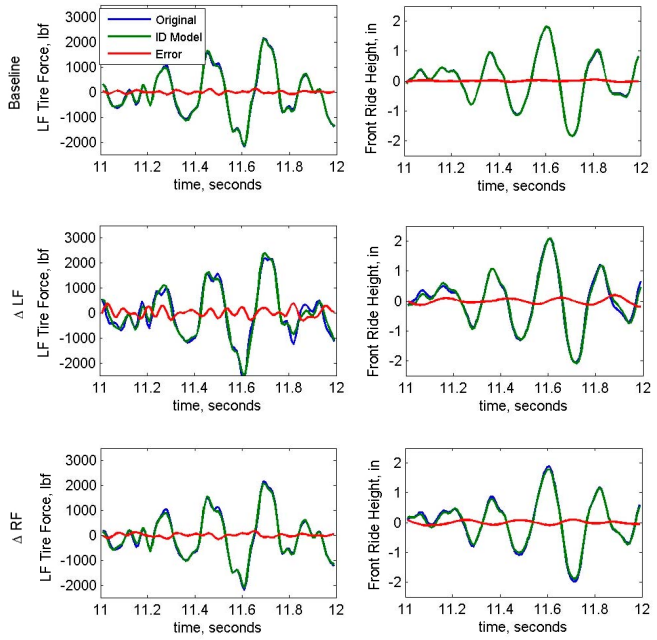

Figure 10. Simulation time trace comparison

The error can be analyzed in further detail in the frequency domain. Figure 11 shows the power spectral density (PSD) for the time signals in Figure 10. For the ride height, the error is 50 dB lower than the signal level. For the tire force, the error is more than 20 dB lower than the signal level, except for the change in left front shock from 7 to 17 Hz. In this frequency band, the peak error is 40 dB lower than the peak signal level, indicating there is limited output energy in this frequency range.

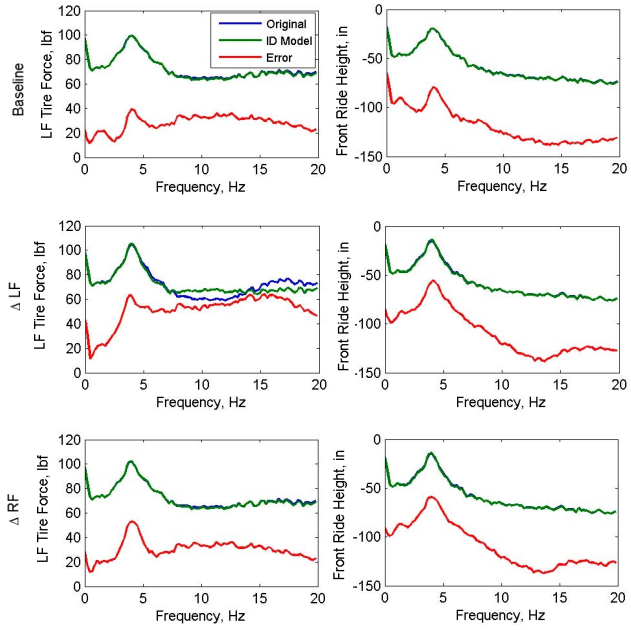

Figure 11. Simulation PSD comparison

The main purpose of this model is to accurately predict trends in response measures as shock setups change. Since the PSDs for the ideal simulation and the ID simulation match well, we would expect RMS response metrics to match well. This is the case, as Figure 12 illustrates.

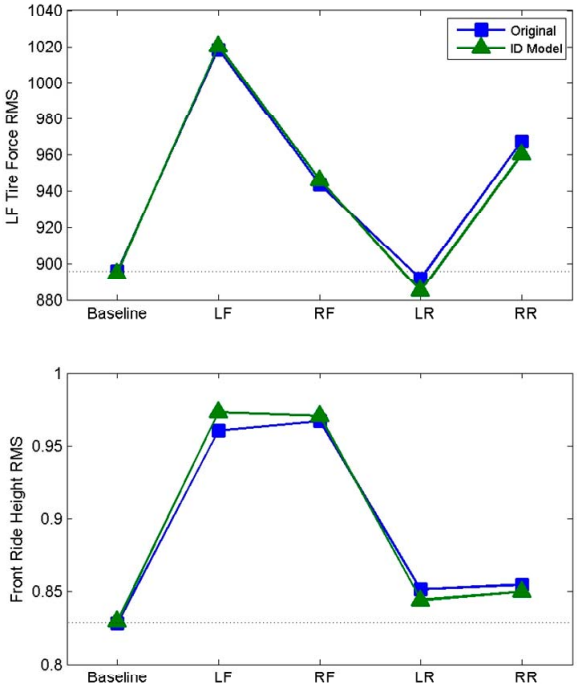

Figure 12. Metric comparison

SUMMARY

This paper has developed a method to identify a linear full-vehicle model from sensor measurements collected during vehicle testing that allows investigation of the effect of shock selection in simulation. To develop the method, a seven degree of freedom vehicle state space model was constructed to generate data sets for the identification process. The identification process can then be judged acceptable if the identified model is similar to the known ideal model.

The frequency response function (FRF) of the state space model was then explored to provide insight prior to the identification process. This analysis showed the importance of both the aeroloaders and the wheelloaders to excite shock velocity at low and high frequencies, respectively. It also showed frequency ranges where we might expect to have poor coherence for certain input/output pairs due to low signal levels.

When the shock force is almost linearly dependent on the wheelloader and aeroloader inputs, the typical FRF estimation process will fail. A modified FRF estimation process was described which uses test data from several different shock configurations to address the shock force dependence issue. This method provided FRF estimates, which matched the ideal FRF where the coherence was high. When the coherence was poor due to low shock force or output levels at low or high frequency, the FRF estimate was replaced by a residual fit with a linear phase and a linear dB/decade rolloff. The FRF estimate was further smoothed by applying a filter, reducing FRF variations with a width of 0.6 Hz or less.

Once an acceptable FRF estimate was calculated, a parametric model was identified by fitting transfer functions to each input-output pair. This parametric model was then be implemented in Simulink using nonlinear dynamic shock models. Simulations were run for 5 different shock configurations and compared to simulation results from the ideal model, showing that the identified model could accurately reproduce the original response and predict trends in response metrics.

Now that this identification process has been shown to accurately reproduce the true system behavior, it can now be applied to data collected from actual 8-post rig testing.

REFERENCES

1. Kelly, J. Kowalczyk, H. Oral, H. Track Simulation and Vehicle Characterization with 7 Post Testing. SAE Technical Papers 2002-01-3307.

2. Kowalczyk, H. Damper Tuning with the use of a Seven Post Shaker Rig. SAE Technical Papers 2002-01-0804.

3. Kasprzak, J. Floyd, R. Use of Simulation to Tune Race Car Dampers. SAE Technical Papers 942504.

4. Vilela, D. Vehicle Dynamics Simulation Correlation with Field Maneuvers. SAE Technical Papers 2001-01-3799.

5. Dittman, K. Albright, F. Leser, C. Validation of Virtual Prototypes via a Virtual Test Laboratory. MTS White Paper.

6. Hu, H. Experimental Validation of a Half-Vehicle Suspension Model. SAE Technical Papers 931966.

7. Ballard, R. Overview of Emerging Technology for Laboratory Based Measurement of Vehicle Performance. SAE Technical Papers 921068.

8. Cheli, F. Sabbioni, E. A Dynamic Light-Duty Vehicle Model: Validation with Indoor and Outdoor Experimental Tests. Proceedings of the ASME 2007 IDETC/CIE 2007, DETC2007-34753.

9. Ziegenmeyer, J. Estimation of Disturbance Inputs to a Tire Coupled Quarter-Car Suspension Test Rig. Master's Thesis, Virginia Tech, May 2007.

10. Boggs, C., Ahmadian, M., and Southward, S., “Application of System Identification for Efficient Suspension Tuning in High-Performance Vehicles: Quarter-Car Study”. *SAE Int. J. Passeng. Cars - Mech. Syst.* **1**(1):1298-1310, 2008.

11. Boggs, C. Ahmadian, M. Efficient Empirical Modeling of a High-Performance Shock Absorber for Vehicle Dynamics Studies. SAE 2007 Transactions Journal of Passenger Cars: Mechanical Systems.

12. Ljung, L. System Identification: Theory for the User. Prentice Hall, 1999. 33.

13. MATLAB R2006b Documentation.